

# Characteristics of spectral aerosol optical depths over India during ICARB

S NASEEMA BEEGUM<sup>1</sup>, K KRISHNA MOORTHY<sup>1</sup>, VIJAYAKUMAR S NAIR<sup>1</sup>, S SURESH BABU<sup>1</sup>,  
S K SATHEESH<sup>2</sup>, V VINOJ<sup>2</sup>, R RAMAKRISHNA REDDY<sup>3</sup>, K RAMA GOPAL<sup>3</sup>,  
K V S BADARINATH<sup>4</sup>, K NIRANJAN<sup>5</sup>, SANTOSH KUMAR PANDEY<sup>6</sup>, M BEHERA<sup>7</sup>,  
A JEYARAM<sup>7</sup>, P K BHUYAN<sup>8</sup>, M M GOGOI<sup>8</sup>, SACCHIDANAND SINGH<sup>9</sup>, P PANT<sup>10</sup>,  
U C DUMKA<sup>10</sup>, YOGESH KANT<sup>11</sup>, J C KUNIYAL<sup>12</sup> and DARSHAN SINGH<sup>13</sup>

<sup>1</sup>Space Physics Laboratory, Vikram Sarabhai Space Centre, Thiruvananthapuram 695 022, India.

<sup>2</sup>Centre of Atmospheric and Oceanic Sciences, Indian Institute of Science, Bangalore 560 012, India.

<sup>3</sup>Department of Physics, Sri Krishnadevaray University, Anantapur 515 003, India.

<sup>4</sup>National Remote Sensing Agency, Balanagar, Hyderabad 500 037, India.

<sup>5</sup>Department of Physics, Andhra University, Visakhapatnam 530 003, India.

<sup>6</sup>ISTRAC Ground Station, Dolly Gunj, Port Blair 744 101, India.

<sup>7</sup>Regional Remote Sensing Service Centre, Indian Institute of Technology Campus, Kharagpur 721 302, India.

<sup>8</sup>Department of Physics, Dibrugarh University, Dibrugarh 786 004, India.

<sup>9</sup>National Physical Laboratory, Dr. K S Krishnan Marg, New Delhi 110 012, India.

<sup>10</sup>Aryabhata Research Institute of Observational Sciences, Nainital 263 129, India.

<sup>11</sup>Indian Institute of Remote Sensing, Dehra Dun 248 001, India.

<sup>12</sup>GB Pant Institute for Himalayan Environment and Development, Manali, Mohal-Kullu 175 126, India.

<sup>13</sup>Department of Physics, Punjabi University, Patiala 147 002, India.

Spectral aerosol optical depth (AOD) measurements, carried out regularly from a network of observatories spread over the Indian mainland and adjoining islands in the Bay of Bengal and Arabian Sea, are used to examine the spatio-temporal and spectral variations during the period of ICARB (March to May 2006). The AODs and the derived Ångström parameters showed considerable variations across India during the above period. While at the southern peninsular stations the AODs decreased towards May after a peak in April, in the north Indian regions they increased continuously from March to May. The Ångström coefficients suggested enhanced coarse mode loading in the north Indian regions, compared to southern India. Nevertheless, as months progressed from March to May, the dominance of coarse mode aerosols increased in the columnar aerosol size spectrum over the entire Indian mainland, maintaining the regional distinctiveness. Compared to the above, the island stations showed considerably low AODs, so too the northeastern station Dibrugarh, indicating the prevalence of cleaner environment. Long-range transport of aerosols from the adjoining regions leads to remarkable changes in the magnitude of the AODs and their wavelength dependencies during March to May. HYSPLIT back-trajectory analysis shows that enhanced long-range transport of aerosols, particularly from the west Asia and northwest coastal India, contributed significantly to the enhancement of AOD and in the flattening of the spectra over entire regions; if it is the peninsular regions and the island Minicoy are more impacted in April, the north Indian regions including the Indo Gangetic Plain get affected the most during May, with the AODs soaring as high as 1.0 at 500 nm. Over the islands, the Ångström exponent ( $\alpha$ ) remained significantly

**Keywords.** Atmospheric aerosols; aerosol optical depth; Ångström parameters; ICARB; long-range transport; multi-wavelength radiometer.

lower ( $\sim 1$ ) over the Arabian Sea compared to Bay of Bengal (BoB) ( $\sim 1.4$ ) as revealed by the data respectively from Minicoy and Port Blair. Occurrences of higher values of  $\alpha$ , showing dominance of accumulation mode aerosols, over BoB are associated well with the advection, above the boundary layer, of fine particles from the east Asian region during March and April. The change in the air mass to marine in May results in a rapid decrease in  $\alpha$  over the BoB.

## 1. Introduction

Aerosols, natural and anthropogenic, affect the climate directly as well as indirectly; though the magnitudes remain uncertain even today (IPCC 2007). The direct effects are due to the absorption and scattering of solar radiation by aerosols leading to changes in the planetary albedo and hence the radiation budget (Charlson *et al* 1992). In the indirect effect, aerosols change the size and number density of cloud droplets, modify the cloud albedo, cloud lifetime and hence the precipitation (Twomey 1977; Albrecht 1989; Rosefield 2000). While scattering (e.g., by sulfate aerosols) results in an increase in atmospheric albedo and a consequent decrease in the amount of radiation reaching the earth's surface (thereby causing a cooling effect (Charlson 1992)), aerosols, such as black carbon (BC) and dust, significantly absorb in the visible and IR spectrum leading to atmospheric warming and a surface cooling. The IPCC (2007) estimates of direct radiative forcing of black carbon aerosols from fossil fuel and biomass burning are in the range of  $+0.27$  to  $+0.54 \text{ Wm}^{-2}$  and for organic carbon they are in the range of  $-0.04$  to  $-0.41 \text{ Wm}^{-2}$ . For dust aerosols the radiative forcing estimates are in the range of  $-2.0$  to  $+0.5 \text{ Wm}^{-2}$  (IPCC 2007).

In assessing the radiative forcing due to aerosols over a given region, the single parameter of utmost importance is the spectral aerosol optical depth (AOD), which is the total extinction caused by aerosols present in a vertical column of the atmosphere. As such, quantifying the magnitude and the spectral variation of AODs is of immense importance not only in understanding our aerosol environment, but also in impact assessment. The sources and sinks of atmospheric aerosols being diverse and scattered in nature, aerosol properties show large spatio-temporal heterogeneity. This is particularly the case with India with its large density of population, its diverse living habits, distinct topographical features, and above all, the large-scale synoptic changes in the prevailing meteorology associated with the monsoon. Despite, there is a scarcity of spatially resolved information on aerosol properties for the Indian regions. One of the goals of the Integrated Campaign for Aerosols, gases and Radiation Budget (ICARB) was to

examine this heterogeneity and its change with time.

As a part of Indian Space Research Organization's Geosphere Biosphere Program (ISRO-GBP), the multi-platform field experiment ICARB was conducted during March to May of 2006. During this period campaign mode observations of aerosol parameters were made over the land, ocean, and in the atmosphere using a variety of instruments on different platforms (Moorthy *et al* 2006). Of these, the land segment has a special importance owing to the fixed nature of the observing station and the consequent capability to provide a time series of the parameters concerned, while the mobile platforms make spatially resolved measurements. During ICARB, spectral aerosol optical depth (AOD) measurements were carried out from 14 land stations, spread over India (figure 1), out of which 12 stations were over the mainland and one each on two islands; Minicoy (MCY) in the Arabian Sea and Port Blair (PBR) in the Bay of Bengal (BoB). The data from these stations for the period March to May 2006 are used to characterise the AODs during ICARB and the results are presented in this paper.

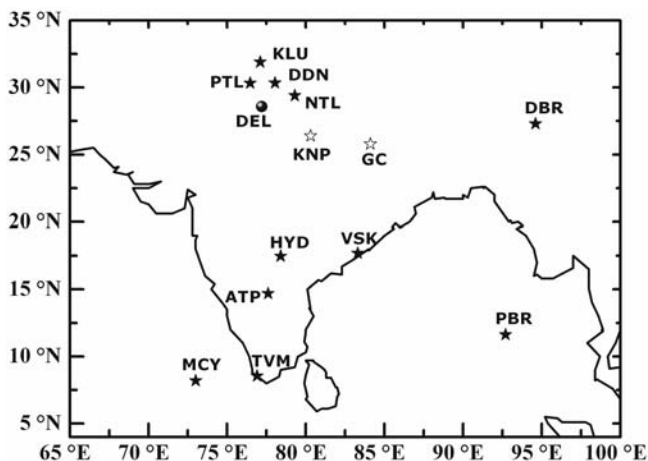


Figure 1. Spatial distribution of the network stations during ICARB. The filled stars denote land stations with MWR observations; the dot represents the station with Microtops observations and the unfilled stars represent the data from the two AERONET stations. Details are given in the text.

## 2. Measurement techniques and details of data

During ICARB, regular measurements of AOD were made using three different instruments; the 10-channel multi-wavelength radiometer (MWR), the 5-channel microtops sun photometer, and the 8-channel CIMEL sun photometer. The MWR (Moorthy *et al* 1997, 1999; Moorthy and Satheesh 2000) estimated AODs at ten wavelength bands centered at 380, 400, 450, 500, 600, 650, 750, 850, 935, 1025 nm (full width half maximum bandwidth of 5 nm and field-of-view of  $2^\circ$ ) following the conventional Langley plot technique (e.g., Shaw *et al* 1973). The estimated spectral AODs correspond to the daily mean or means for the forenoon and afternoon (FN and AN) parts of the same day, whenever the Langley plots showed a change in the slope from the FN to AN. This instrument was operated from eleven stations; Minicoy ( $8.2^\circ\text{N}$ ,  $73.0^\circ\text{E}$ , 1 m msl, MCY), Port Blair ( $11.63^\circ\text{N}$ ,  $92.7^\circ\text{E}$ , 73 m msl, PBR), Trivandrum ( $8.55^\circ\text{N}$ ,  $76.9^\circ\text{E}$ , 3 m msl, TVM), Anantapur ( $14.7^\circ\text{N}$ ,  $77.6^\circ\text{E}$ , 331 m msl, ATP), Hyderabad ( $17.48^\circ\text{N}$ ,  $78.4^\circ\text{E}$ , 545 m msl, HYD), Visakhapatnam ( $17.7^\circ\text{N}$ ,  $83.3^\circ\text{E}$ , 5 m msl, VSK), Dibrugarh ( $27.3^\circ\text{N}$ ,  $94.6^\circ\text{E}$ , 104 m msl, DBR), Nainital ( $29.2^\circ\text{N}$ ,  $79.3^\circ\text{E}$ , 1950 m msl, NTL), Patiala ( $30.33^\circ\text{N}$ ,  $76.46^\circ\text{E}$ , 251 m msl, PTL), Dehra Dun ( $30.34^\circ\text{N}$ ,  $78.04^\circ\text{E}$ , 690 m msl, DDN) and Kullu ( $31.9^\circ\text{N}$ ,  $77.1^\circ\text{E}$ , 1155 m msl, KLU), where msl stands for the station altitude above mean sea level. Typical uncertainties in the AODs retrieved from the MWR varied between 0.02 and 0.03 (Moorthy *et al* 1997). Trivandrum is a rural, coastal location on the west coast of the southern tip of India; Anantapur is a rural semi-arid location and Hyderabad an urban, industrial location (both in central peninsula), while Visakhapatnam is an industrialized coastal location on the east coast of India. In the north, we have Dibrugarh, a rural clean location on the far eastern part of India; Nainital, a high altitude location (2 km above msl) in the western part of the Himalayas; Patiala, an urban location in Punjab; Dehra Dun, an elevated station at the Himalayan foothills and about 200 km north of the megacity Delhi; and Kullu, a high altitude Himalayan region north of Nainital. The MWRs used in all the above stations were identical and data were collected during clear sky days and partially cloudy days, when the region of sky of  $\sim 10^\circ$  around the sun is free from clouds. Effects of patches of clouds are removed by screening of the data using a Student 't' statistics of 0.99 confidence coefficients. More details on the MWR data analysis and error budget are given in Saha and Moorthy (2005). The data collection and analysis have been carried out following a common protocol.

The Microtops (Solar Light Company, USA) is a hand-held sun photometer that provides AOD and columnar water vapour from instantaneous measurements, based on its internal calibrations, at five channels (340, 500, 670, 936 and 1020 nm). The full-width half-maximum bandwidth ranged from 2.4 nm in the UV to 10 nm at visible and near IR wavelengths. Details of the instrument and data collection protocols are available in the literature (Morys *et al* 2001; Ichoku *et al* 2002; Porter *et al* 2001). The main errors in the Microtops, apart from errors due to cloud contamination, include inaccurate pointing to the sun, and neglecting to clean the front quartz window. These issues were adequately taken care of while collecting the data. During the land segment of the ICARB this instrument was operated from Delhi ( $28.58^\circ\text{N}$ ,  $77.2^\circ\text{E}$ , 260 m msl, DEL), the highly populated capital city of India, and from Kullu during March 2006. Each time, a set of three measurements were made in quick succession after pointing the instrument to the sun, and least of these is taken as the AOD at that time.

Besides these, the CIMEL sun photometer was in operation from two Indian stations, the Indian Institute of Technology (IIT) Kanpur ( $26.4^\circ\text{N}$ ,  $80.3^\circ\text{E}$ , 142 m msl, KNP), an industrial site in the Indo-Gangetic Plains (IGP); and from Gandhi College Campus ( $25.8^\circ\text{N}$ ,  $84.1^\circ\text{E}$ , 64 m msl, GC), a rural village location, as a part of the AERONET (AEROSOL ROBOTIC NETWORK) program (Holben *et al* 1998). The instrument provided instantaneous AOD at eight spectral channels (340, 380, 440, 500, 675, 870 and 1020 nm) (based on its internal calibration), columnar water vapour content and several other derived parameters such as size distribution, phase function, and single scattering Albedo (Holben *et al* 1998). The uncertainty in the retrieved AOD under cloud free conditions is 0.01 to 0.02. The level 1.5 data (<http://aeronet.gsfc.nasa.gov>) from these stations are used after removing the outliers (values lying beyond the  $2\sigma$  level,  $\sigma$  being the standard deviation).

## 3. Prevailing meteorology

The synoptic winds during the ICARB period (March–May 2006) are shown in figure 2 at 850 hPa level, based on the NCEP/NCAR reanalysis data. It is seen that, over the Indian land-mass and adjoining oceans, the winds are mostly weak ( $< 3 \text{ ms}^{-1}$ ) during March. The speed increases gradually towards April and in May, strong westerlies are established. A high-pressure region, located over the peninsula (at  $15^\circ\text{N}$ ) during March–April months, results in a weak anticyclonic circulation

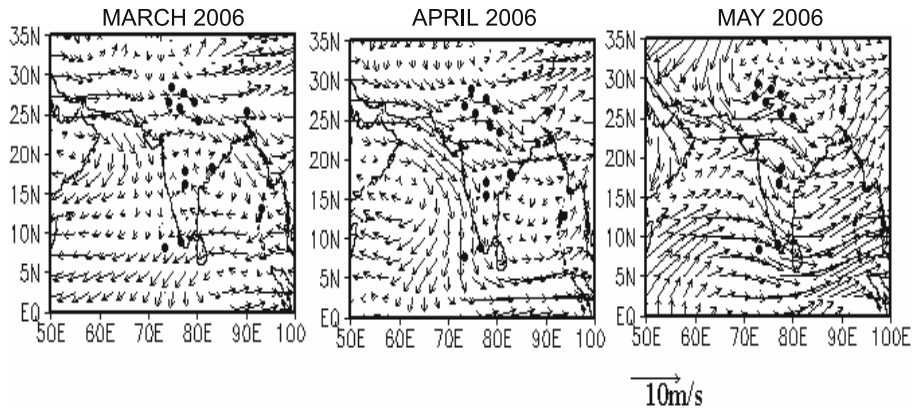


Figure 2. Monthly mean wind vectors (from NCEP data) at 850 hPa for March, April and May 2006 over the study regions. The black dots represent the land stations having observations during the period.

as seen in figure 2. This high pressure disappears in May. Over Port Blair, the northeasterly winds of March change to southwesterlies in May. The observed pattern is in general conformity to the climatological pattern (Asnani 1993).

## 4. Results and discussion

### 4.1 Aerosol Optical Depth

Daily mean spectral AODs were estimated for the fourteen stations (mentioned above) over India. For the AERONET stations and stations with Microtops observations, the daily averages were estimated by averaging out all the measurements during the day. These daily averaged AOD formed the basic data, from these, the corresponding monthly mean spectral AODs were calculated by grouping all the daily mean spectral AOD values into calendar months and averaging. Mass plots of the monthly mean AOD spectra are shown in figures 3 to 5, respectively for the months of March, April and May 2006. The vertical bars through the points in the figures represent the standard errors. The main findings are listed below:

- During March, high AODs occur over the peninsular India, with ATP, HYD and TVM topping the list. Moderate levels of AODs are seen at the IGP stations (Indo-Gangetic Plain) DEL, DDN, and KNP. While DBR lies between these two sets, station MCY shows moderately high AODs comparable to those at the IGP stations. Low AODs, particularly at mid-visible and near IR wavelengths are seen at VSK and the eastern island station PBR. The high altitude stations of NTL and KLU, and the northwestern station PTL show extremely low AODs. By April, the AODs register substantial increase at all the

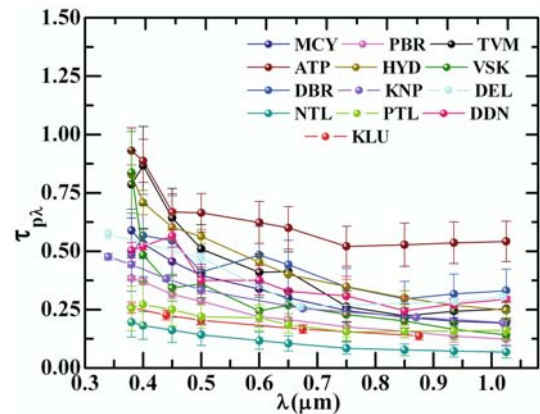


Figure 3. The monthly mean spectral variations of AOD for different land stations during March 2006.

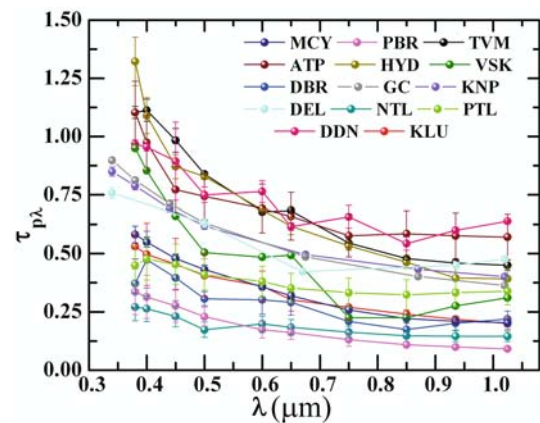


Figure 4. Same as figure 3, but for the month of April 2006.

stations, even though the quantum of increase varied. The increase was more at the western IGP stations, so that AODs at DEL and DDN become comparable to those at ATP and TVM, with HYD (AOD at 500 nm > 0.8) topping the

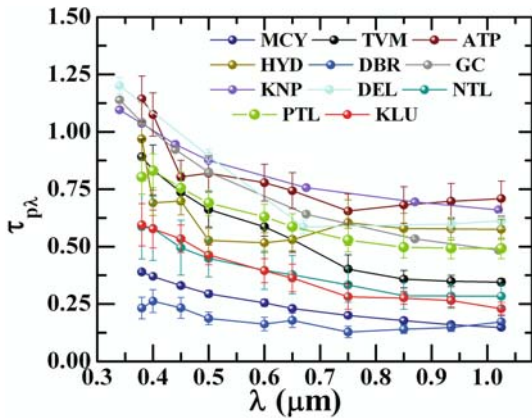


Figure 5. Same as figure 3, but for the month of May 2006.

list. Even KLU and PTL register a significant increase and surpass DBR and PBR, while NTL continues to remain at the lowest, even though this lowest is higher than that seen in March. As we enter May, AODs shoot-up at all the IGP stations and DEL (AOD 0.9 at 500 nm), KNP, and GC top the list along with ATP. At PTL, the AODs become moderately high, and even at KLU and NTL the AODs become comparable to or just below TVM and HYD. MCY and DBR register the lowest AODs for May.

- Despite the general pattern described above, the AOD spectra show considerable spatio-temporal variations. Generally the spectra tend to be steeper in the peninsular regions, implying more abundance of accumulation-sized particles. The steepness decreases from March to May suggesting a change in the aerosol size spectrum with increased coarse mode domination.

To get a snap shot of the spatio-temporal characteristics, we show, in figure 6, the contour map of AOD at 500 nm for March, April, and May in panels respectively from left to right at the top; (a, b and c). In doing so, a spatial homogeneity for approximately  $1^\circ$  radius about the observing station was assumed. The figure 6(a–c) shows that, the island stations as well as the NE station DBR, show less pronounced temporal variations. This is attributed to (a) the isolated nature of the islands and the low level of anthropogenic activities on them, and (b) the tall Himalayan ranges surrounding DBR, which restrict transport of aerosols from the adjoining regions. At these places, the AOD decrease towards May. In contrast to this, the peninsular India shows a sharp increase from March to April, before starting to decrease in May. The peaking of aerosol optical depth in April over the peninsular stations is in general conformity with the climatological pattern reported for this region (Moorthy *et al* 1999). The prevailing

weak, and anticyclonic, low-level winds (figure 2) contribute to this by confining the aerosols spatially, while the weak removal mechanism (insignificant rainfall) is conducive for a longer lifetime of aerosols. In the IGP region, there is a continuous increase in the AOD from March to May; and in May this region has the highest AOD. The impact of this increase is seen even on the central Himalayan region also. This is attributed mostly to (i) picking up of dust particles in the locality by the strong convective eddies resulting from the intense heating of the land (a meso-scale feature), and (ii) the long-range transport of aerosols (mostly dust) from the arid region of west Asia and western India across the IGP (e.g., Moorthy *et al* 2007). Consequently, the composition and size distribution of aerosol undergo changes, which get reflected in the AOD spectra. To examine this aspect, we estimated the Ångström parameters.

#### 4.2 Ångström parameters

The Ångström parameters, the wavelength exponent  $\alpha$  and turbidity coefficient  $\beta$  in the equation  $\tau_{p\lambda} = \beta\lambda^{-\alpha}$  (Ångström 1964), are estimated from the individual day AOD spectra (by performing a regression analysis between the wavelength  $\lambda$  in micrometer and the AOD, both in log-log scale, for the entire spectral range of measurement) and the average spatial distribution are examined in figure 6(d–f) (middle row) for the individual months. The figure reveals that:

- In the southern and central peninsular regions,  $\alpha$  is generally high (in the range 1 to 1.4), the higher values occur during March and over industrialized/urban locations (e.g., HYD and VSK). Nevertheless, they are high ( $\sim 1.2$ ) even at the island stations (MCY and PBR) and also at TVM. Over the peninsula, only ATP shows lower values of  $\alpha$ .
- Coming to the northern Indian regions, the high altitude stations of NTL, DDN and KLU show higher values of  $\alpha$  in March compared to the stations in the IGP (PTL, DEL, KNP and GC), probably because of the reduced abundance of coarse mode aerosols at the higher elevations.
- As the months progress from March to May,  $\alpha$  decreases at all the stations; the decrease being more conspicuous over the IGP and Himalayan regions.
- The northeast station DBR shows an increase in  $\alpha$  from March to April followed by a decrease in May.

The spatial pattern of turbidity coefficient  $\beta$  (figure 6(g–i) bottom panel), which is the measure

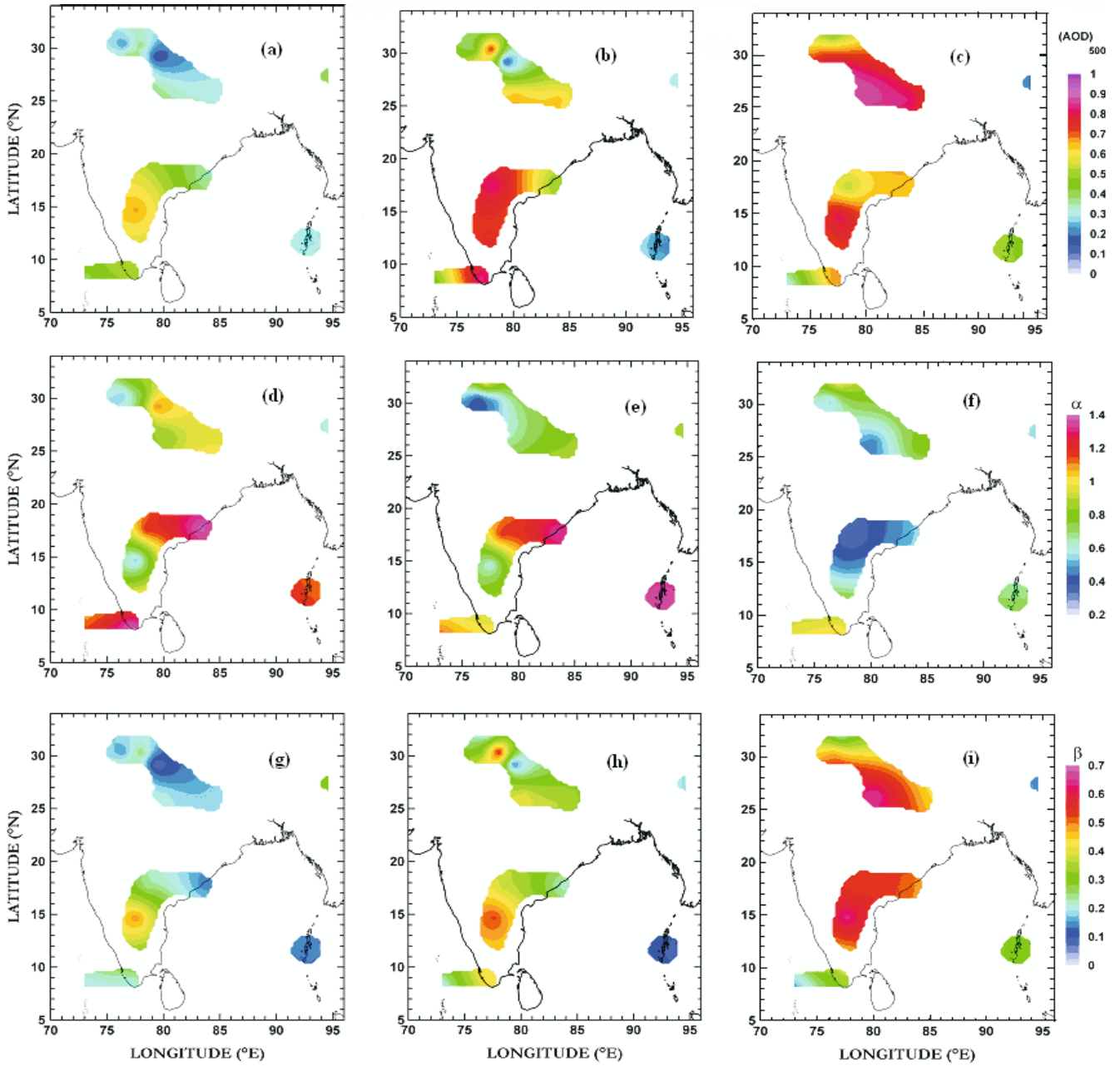


Figure 6. Spatial distribution of monthly mean aerosol optical depth at 500 nm (a–c); Ångström wavelength exponents (d–f) and turbidity coefficient (g–i) over Indian subcontinent from March to May.

of the column abundance of aerosols, is quite similar to that of AOD. Very low values of  $\beta$  prevail over the island stations although the period, with very little temporal changes. In the southern peninsula, on the other hand,  $\beta$  remarkably increases in April, followed by a weak decrease in May. In the central peninsular stations, however, the increasing trend continues until May. In the north, at the IGP stations KNP, GC, and DEL,  $\beta$  increases gradually from March to reach very high values in May. In May,  $\beta$  is as high as 0.6 for KNP and 0.5 for DEL. This feature is seen even at the high

altitude stations of KLU and NTL. Interestingly, the northeast station, DBR, shows very low loading with a moderate value ( $\sim 0.3$ ) of  $\beta$  in March, which decreases through April to reach  $\sim 0.15$  by May.

#### 4.3 Long-range transport

Long-range transport of aerosols from adjoining regions is known to modify the aerosol properties at several regions over India (e.g., Moorthy *et al* 2003, 2005). In order to examine this in

Table 1. Trajectory-groups and details of advection for the mainland stations.

Trajectory group	Origin/regions covered	Short form	Color of the Pie segment in figure 8 (a, b, c)
I	From Bay of Bengal, across or around the southern peninsular India (considered as polluted marine airmass)	BoB	Red
II	From the Arabian Sea, without significant continental travel (mostly marine)	AS	Green
III	Confined to central north India and Indo-Gangetic Plain	CI	Blue
IV	From central peninsular India	CP	Cyan
V	From west Asia, across Afghanistan, Pakistan and northwest India/western coastal India	WA	Magenta

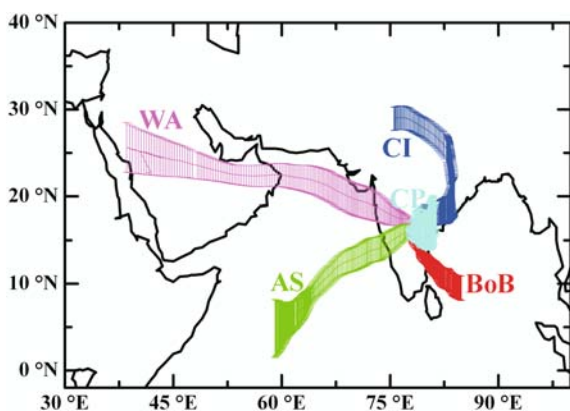


Figure 7. Airmass back trajectories, grouped according to the regions covered, and arriving at 1800 m msl over HYD (representative of the mainland location) for the month of March. The vertical bars over the mean line show the spatial spread of each group. Details are given in the text and table 1.

causing the observed temporal changes in AOD, we computed the 7-day isentropic airmass back trajectories using Hybrid Single Particle Lagrangian Interpolated Trajectory (HYSPLIT) model at all the network stations for the days of AOD measurements. As the AODs are contributed by the particles in the entire atmospheric column, we considered 3 levels at each stations: one at 500 m (well within the Atmospheric Boundary Layer (ABL)); second at 1800 m (mostly above the ABL; but below the trade wind inversion layer); and the third at 3600 m, in the free troposphere, following the criteria given in Moorthy *et al* (2005). The 7-day period was considered for the trajectories in view of the long atmospheric lifetime (more than a week) for the particles in the absence of wet removal (Jaenicke 1984; Babu and Moorthy 2002).

#### 4.3.1 Mainland stations

Based on a careful examination, we grouped the entire trajectories into 5 groups for the mainland locations (as listed in table 1), depending on the regions traversed by the trajectories, and the percentage share (to the total) of each group was determined. An illustrative example of the different trajectory groups considered at (1800 m) level in March at HYD, is shown in figure 7, where the trajectory groups are identified following the conventions used in table 1. An interesting feature is that while the trajectories pertaining to group V have a long continental travel over the arid/semi-arid regions during the 7 days, those in group VI (CP) are confined locally. The summary of this exercise are given in figure 8(a-c) respectively for three representative locations; (a) TVM, at the southern tip of the peninsula; (b) Hyderabad, central peninsula; and (c) DEL in the IGP region; all the stations lying almost along the same longitude. Each figure has 9 pie diagrams showing the month wise and altitudewise summary of long-range transport. Each segment of the pie corresponds to a particular trajectory group (table 1) and the area of each segment (of the pie) corresponds to the percentage contribution of that group to the total.

The figures very clearly reveal that the large increase in AOD seen in the peninsular region in April, and the associated increase in  $\beta$  and decrease in  $\alpha$ , are closely associated with the increase in the percentage contribution of advection from the west Asia and west coastal India (trajectory group V). Though the increase is seen at all the three levels, it is more conspicuous at the higher levels. By May, the pattern changes dramatically with a large share coming from the Arabian Sea (trajectory group II), at the expense of group V. This results

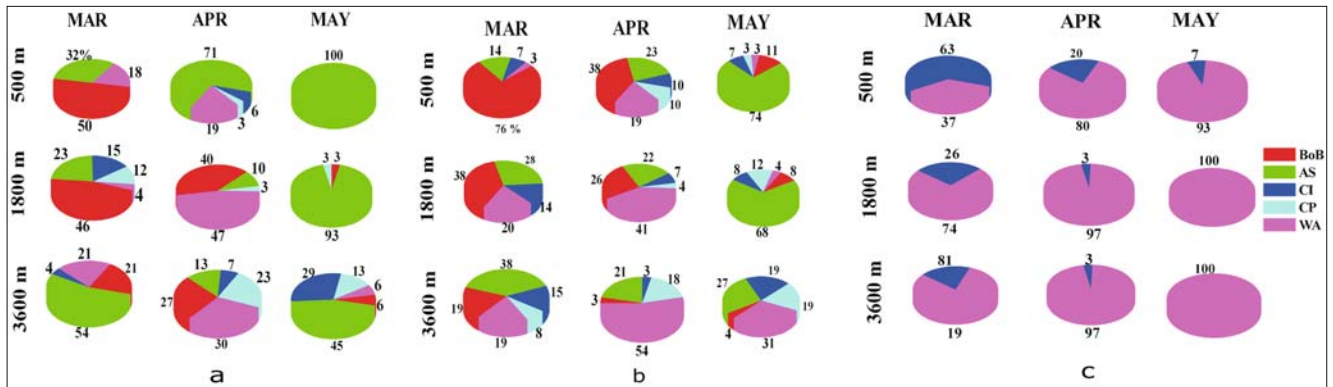


Figure 8. Pie-chart representation of the percentage contribution from different groups of trajectories described in table 1, for the three altitude regions 500 m, 1800 m and 3600 m for March, April and May over three stations: TVM (a) representative of southern peninsular India, HYD (b) central Peninsula, and DEL (c) the Indo Gangetic Plain.

Table 2. Trajectories group and details of advection for the island stations.

Origin/regions covered	Trajectory group name	Color of the Pie segment in figure 8 (a and b)
From west Asia, across Afghanistan and north-west India/western coastal India	W	Magenta
From the subcontinent of India	I	Blue
From east Asia	E	Dark red
From the Arabian Sea and Bay of Bengal, without any continental proximity (mostly pure marine)	M	Dark yellow

in a decrease not only in the AOD and  $\beta$ , but in  $\alpha$  also as the marine air mass would be dominated by coarse mode particles. The low AOD and high  $\alpha$  seen in March is mainly attributed to the significant contribution of the advected air mass belonging to trajectory group I (arriving across the BoB) bringing-in fine, accumulation aerosols. It may be recalled that such observations of low AOD and high  $\alpha$  are reported earlier also, associated with advection from the BoB (Moorthy *et al* 2005).

Going to the north, the major share to the advection comes from two groups of trajectories (III and V), which arrive from the central India and west Asia respectively. The percentage contribution of the west Asian group (group V) keeps increasing steadily from March and by May, it prevails totally over the region. As this air mass traverses vast desert and arid regions, they would be rich in coarse dust aerosols, which contribute to the observed features; such as increase in AOD and  $\beta$  and decrease in  $\alpha$ . It may also be recalled that based on observations from Jodhpur, further west of these station, Moorthy *et al* (2007) have reported large increase in the AOD during summer and even a reversal in the spectral depen-

dence. They have identified this to the dominance of nascent dust particles in the atmosphere. Based on their investigations from KNP, Dey *et al* (2004); Singh *et al* (2004); and Chinnam *et al* (2006), have reported that soil dust is an important source of aerosols during pre-monsoon and monsoon seasons. Chinnam *et al* (2006) have identified three major sources of mineral dusts (mixed with anthropogenic pollutants) during this period: (1) from Oman, (2) from southwest Asian basins, and (3) from Thar Desert in Rajasthan. Recent studies by Tare *et al* (2006) on the PM and BC emissions in the vicinity of Kanpur have shown three major sources: the soil derived, those from biomass burning, and those from gas-phase reaction products; the contribution of soil-derived components being significant in the coarse mode (diameter 0.95–10  $\mu\text{m}$ ) regime.

#### 4.3.2 Island locations

For the island locations of PBR and MCY, we grouped the trajectories into 4 groups, as given below in table 2 following the same procedure for the mainland stations. The logic of the grouping

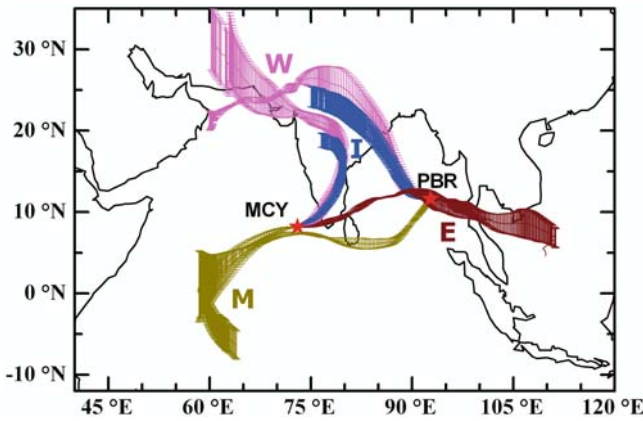


Figure 9. Back trajectory groups arriving at the 1800 msl over MCY and PBR for the month of April. The vertical bars over the mean line show the spatial spread of each group. Details of grouping the trajectories are given in the text and table 2.

of the trajectories as described in the table 2, is evident from the representative plot for the month of April shown in figure 9 for the two stations (PBR and MCY). In the figure the average trajectories arriving at the respective locations at 1800 m level are shown and the vertical bars over the mean line show the spatial spread of each group (represented by the respective ensemble standard deviation). The summary of the analysis is given in figure 10(a and b) respectively for three representative altitudes for (a) Minicoy in Arabian Sea and (b) Port Blair in the Bay of Bengal (following similar convention in figure 7).

Moderately high values of AOD,  $\beta$  in Minicoy for the month of March (figure 10a) are closely

associated with the high percentage contribution to the advection by the trajectory (group W), which is more conspicuous at the low level, while at the levels of 1800 m and 3600 m all the trajectory groups contribute almost equally. This leads to moderately high AOD and  $\alpha$  ( $\geq 1$ ). In April, even though a small increase in AOD and  $\beta$  are observed, the  $\alpha$  remained more or less the same. This increase in AOD and  $\beta$  can be attributed to the further increase in the share of W, which now contributed  $>90\%$  to the total at lower levels, whereas at the higher level (3600 m), the trajectories group I from the Indian subcontinent is contributed significantly. This ‘mixed trajectories’ led to the high AOD and moderate  $\alpha$ . Such observations of enhanced dust transport over Arabian Sea from the Arabian and African continents were reported earlier (e.g., Li and Ramanathan 2002; Moorthy *et al* 2005) during April–May period. In May, the pattern changes with a large share coming from the marine locations (group M) for all the three levels. This results in a (weak) decrease in AOD,  $\beta$  and  $\alpha$ . It might be recalled that several observations over far oceanic regions have shown flat AOD spectra (Hoppel *et al* 1990; Moorthy *et al* 1997) during periods of marine airmasses.

Examining the island location of Port Blair (figure 10b) in the month of March, the major share to the advection at the lower level is from India (group I), while at higher levels the advection from East Asia (group E) dominates. Consequently low values of AOD and  $\beta$  and comparatively higher values ( $> 1$ ) of  $\alpha$  prevail. In April, there is a remarkable increase in the contribution from group E (East Asia) at all the three levels, and  $\alpha$  goes to

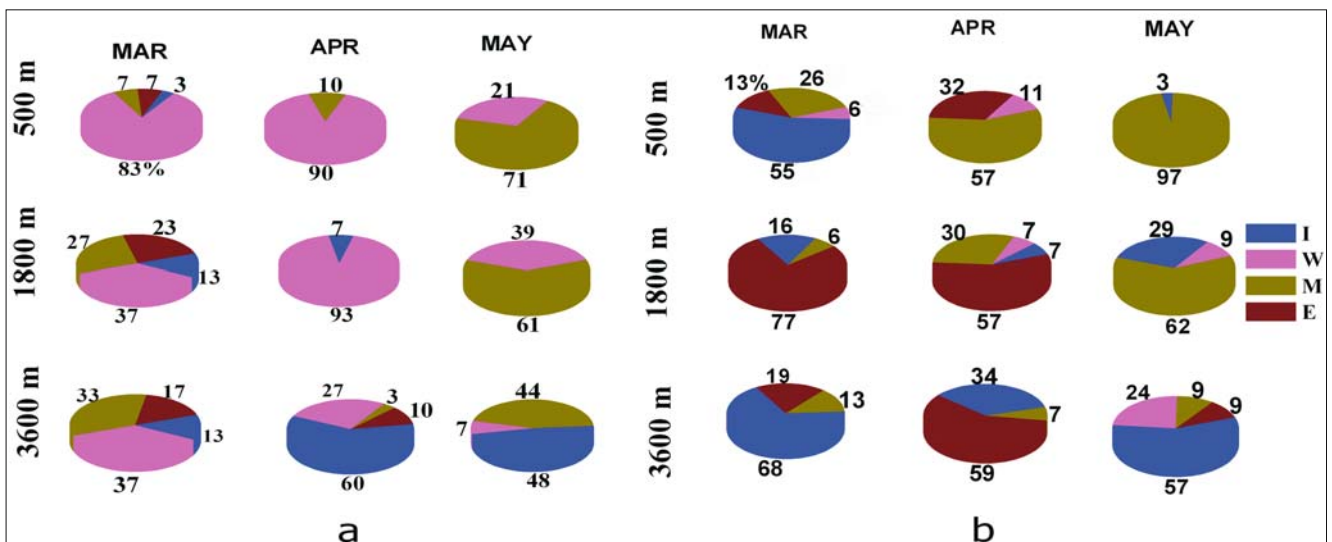


Figure 10. Pie-chart representation of the percentage contribution from different groups of trajectories described in table 2, for the three altitude regions 500 m, 1800 m and 3600 m for March, April and May over the two island stations of MCY (a) and PBR (b).

as high as 1.4. This is in good agreement with the earlier observations for Port Blair by Moorthy *et al* (2003), who reported a steepening of the AOD spectra associated with east Asian transport. They attributed it to the advection of accumulation mode aerosols from the east Asian region. The effect was most dominant when the trajectories at all three levels arrived from the east. Our present observations show that this feature is persistent.

## 5. Conclusions

Our studies during the ICARB using a spatial network of observatories have shown that over the Indian mainland, AODs and the derived Ångström parameters depict large spatio-temporal variations. The major findings are:

- The spectral AODs and  $\beta$  tend to increase continuously from March to May over the entire north India, with the IGP registering extremely high AODs by May. However, over the central peninsular stations, the AODs and  $\beta$  increase from a moderately high value in March to a peak in April followed by a decrease in May.
- As far as the spectral variations are concerned, the southern, peninsular stations show steeper spectra during all the three months corresponding to their north Indian counterparts. Over the entire mainland, the spectra become increasingly flat from March to May. However, at the Himalayan stations, even  $\alpha$  shows similar temporal variations as in the plains, their values are higher.
- In the peninsula, the industrialized and urban locations such as VSK and HYD show higher values of  $\alpha$ , compared to other stations, while the semi-arid station ATP shows a lower value.
- The island stations MCY and PBR as well as the northeastern station DBR, show low values of AOD and  $\beta$ , and show very small temporal variations. Of these, PBR shows steeper spectra. These are attributed to isolated nature of these stations (either detached from the mainland or shielded by the tall mountain ranges) and the reduced human impact. The higher values of  $\alpha$  at PBR are partly attributed to the advection from the east Asian regions.
- Enhanced long-range transport of aerosols, particularly from the west Asia and north west India, contributed significantly to the enhancement of AOD and  $\beta$ , and the decrease of  $\alpha$  over the entire mainland; if it is the peninsular regions that are more impacted in April, the north-Indian region including the Indo Gangetic Plain get affected the most during May. The impact

seems to be more through trajectories arriving at higher levels, than within the boundary layer.

- For the island locations of PBR and MCY too, the long-range transport plays an important role. In MCY, significant advection occurs from the arid regions of Arabia and Africa as well as those from the central peninsular region of India (dominated by accumulation mode particles). This leads to a mixed type of aerosols resulting in high AOD and  $\beta$  and moderate values for  $\alpha$ . However, at PBR, the increased advection from the continental locations of east Asia is responsible for the increased values of  $\alpha$  for the month of April.

## Acknowledgements

The authors acknowledge the technical support received from Mr P Pradeep Kumar and Mr P P Pramod for the entire network activity. The authors thank the NOAA air resources laboratory for the provision of the HYSPLIT transport and dispersion model and READY website (<http://www.arl.noaa.gov/ready.html>). We also acknowledge AERONET team members for data collection and calibration and the website <http://aeronet.gsfc.nasa.gov>.

## References

- Albrecht B A 1989 Aerosols, cloud microphysics and fractional cloudiness; *Science* **245** 1227–1230.
- Ångström A 1964 Techniques of determining the turbidity of the atmosphere; *Tellus* **13** 214.
- Asnani G C 1993 *Tropical Meteorology* 1 603. Indian Inst. of Trop. Meteorol., Pune.
- Babu S S and Moorthy K K 2002 Aerosol black carbon over a tropical coastal station in India; *Geophys. Res. Lett.* **29(23)** 2098, doi:10.1029/2002GL015662, 13–1 to 13–4.
- Charlson R J 1992 Climate forcing by anthropogenic aerosols; *Science* **255** 423–430.
- Chinnam N, Dey S, Tripathi S N and Sharma M 2006 Dust events in Kanpur, Northern India: Chemical evidence for source and implications to radiative forcing; *Geophys. Res. Lett.* **33** L08803, doi:10.1029/2005GL025278.
- Dey S, Tripathi S N, Singh R P and Holben B 2004 Influence of dust storm on the aerosol parameters over the Indo-Gangetic Basin; *J. Geophys. Res.* **109** D20211, doi:10.1029/2004JD004924.
- Holben B N, Eck T F, Slutsker I, Tanre D, Buis J P, Setzer S, Vermote E, Reagan J A, Kaufman Y J, Nakajima T, Lavenu F, Jankowiak I and Smirnov A 1998 AERONET – A federated instrument network and data archive for aerosol characterization; *Rem. Sens. Environ.* **66** 1–16.
- Hoppel W A, Frick G M, Larson R E and Mack E J 1990 Aerosol size distributions and optical properties found in the marine boundary layer over the Atlantic Ocean; *J. Geophys. Res.* **95** 3659–3686.
- Ichoku, Charles, Robert Levy and Kaufman Y J *et al* 2002 Analysis of the performance characteristics of the

- five-channel Microtops II Sun Photometer for measuring aerosol optical thickness and perceptible water vapor; *J. Geophys. Res.* **107(D13)** 10.1029/2001JD00130.
- Intergovernmental Panel on Climate Change 2001; Climate change 1994: Radiative Forcing of Climate, report to IPCC from the Scientific Assessment Group (WGI) (New York: Cambridge Univ. Press).
- Intergovernmental Panel on Climate Change 2007 Climate change – 2007, Changes in Atmospheric Constituents and in radiative Forcing, Contribution of Working group to the Fourth Assessment report of the IPCC (New York: Cambridge Univ. Press).
- Jacobson M Z 2001 Strong radiative heating due to the mixing state of black carbon in atmospheric aerosols; *Nature* **409** 695–697.
- Jaenicke R 1984 Aerosols and their climatic effects; A Deepak Publishing, Virginia, USA.
- Li F and Ramanathan V 2002 Winter to summer monsoon variation of aerosol optical depth over tropical Indian Ocean; *J. Geophys. Res.* **107** doi:10.1029/2001JD000949.
- Moorthy K K and Satheesh S K 2000 Characteristics of aerosols over a remote island, Minicoy in the Arabian Sea: optical properties and retrieved size characteristics; *Quart. J. Roy. Meteorol. Soc.* **126** 81–109.
- Moorthy K K, Satheesh S K and Murthy B V K 1997 Investigations of marine aerosols over the tropical Indian Ocean; *J. Geophys. Res.* **102** 18,827–18,842.
- Moorthy K K, Niranjana K, Narasimha Murthy B N, Agashe V V and Murthy B V K 1999 Aerosol Climatology over India; 1 – ISRO GBP MWR Network and Database, ISRO GBP, ISRO GBP SR-03-99, Indian Space Research Organisation, Bangalore.
- Moorthy K K, Babu S S and Satheesh S K 2003 Aerosol spectral optical depths over the Bay of Bengal: Role of transport; *Geophys. Res. Lett.* **30(5)** 1249, doi:10.1029/2002GL016520.
- Moorthy K K, Babu S S and Satheesh S K 2005 Aerosol characteristics and radiative impacts over the Arabian Sea during the intermonsoon season: Results from ARMEX field campaign; *J. Atmos. Sci.* **62** 192–206.
- Moorthy K K, Satheesh S K and Babu S S 2006 ICARB: An integrated campaign for Aerosols, gases and radiation budget; *Proc. of SPIE* **6408** 64080P, 0277-786X/06/\$15 · doi:10.1117/12.696110.
- Moorthy K K, Babu S S, Satheesh S K, Srinivasan J and Dutt C B S 2007 Dust Absorption over the “Great Indian Desert” inferred using ground-based and satellite remote sensing; *J. Geophys. Res.* **112** D09206, doi:10.1029/2006JD007690.
- Morys M, Mims F M, Hagerup S, Anderson S E, Baker A, Kia J and Walkup T 2001 Design, calibration and performance of MICROTOS II hand-held ozone monitor and Sun Photometer; *J. Geophys. Res.* **106(D13)** 14,573–14,582.
- Porter, John N, Mark Miller, Christophe Pietras and Craig Motell 2001 Ship-Based Sun Photometer Measurements Using Microtops Sun Photometer; *J. Atmos. Ocea. Tech.* **18** 765–774.
- Rosefield D 2000 Suppression of rain and snow by urban and industrial air pollution; *Science* **287** 1793–1796.
- Saha A and Moorthy K K 2005 Interannual Variations of Aerosol Optical Depth over Coastal India: Relation to Synoptic Meteorology; *J. Appl. Meteorol.* **44** 1066–1077.
- Shaw G E, Regan R A and Herman B M 1973 Investigations of atmospheric extinctions using direct solar radiation measurements made with a multiple wavelength radiometer; *J. Appl. Meteorol.* **12** 374–380.
- Singh R P, Dey S, Tripathi S N and Tare V 2004 Variability of aerosol parameters over Kanpur, northern India; *J. Geophys. Res.* **109** D23206, doi:10.1029/2004JD004966.
- Tare V *et al* 2006 Measurement of atmospheric parameters during ISRO-GBP Land Campaign II at a typical location in the Ganga Basin: 2. Chemical properties; *J. Geophys. Res.* **111** D23210, doi:10.1029/2006JD007279.
- Twomey S A 1977 The influence of pollution on the short-wave albedo of clouds; *J. Atmos. Sci.* **34** 1149–1152.